

Adaptive polygon scaled boundary finite element method for elastodynamics

*Z.H. Zhang ¹and Z.J. Yang²

¹College of Civil and Environmental Engineering, Ningbo University, China

²College of Civil Engineering and Architecture, Zhejiang University, China

*Corresponding author: zhangzihua@nbu.edu.cn

Abstract

An adaptive polygon scaled boundary finite element method (APSBFEM) is developed for elastodynamic problems. Flexible polygon meshes are generated from background Delaunay triangular meshes and used to calculate structure's dynamic responses. In each time step, a posteriori-type energy error estimator is employed to locate the polygon subdomains with exceeding spatial discretization error, then edge midpoints of the corresponding triangles are inserted into the background. A new Delaunay triangular mesh and a polygon mesh are regenerated successively. The state variables, including displacement, velocity and acceleration are mapped from the old polygon mesh to the new one by a simple algorithm. A benchmark elastodynamic problem is modeled to validate the developed method. The results show that the adaptive meshes are capable of capturing the steep stress gradient areas, and the dynamic responses agree well with those from the adaptive finite element method and the general polygon scaled boundary finite element method using fine meshes.

Keywords: Adaptive, Scaled Boundary Finite Element Method, Polygon, Elastodynamics, Energy error estimator

Introduction

Spatial discretization error inevitably exists in numerical methods, especially for dynamic problems. In order to limit the discretization error within an acceptable level, adaptive methods can be used to refine the steep stress gradient areas with exceeding error automatically by means of error estimators and remeshing procedures. Adaptive finite element methods (AFEM) [Zeng and Wiberg (1992)] have been developed to seek appropriate spatial discretization with the least computational cost, but the remeshing procedures are complicated and time-consuming, especially for large scale problems. Furthermore, mesh mapping after remeshing to transfer state variables from the old mesh to the new one is approximate in FEM, leading to high accumulative errors in subsequent time steps.

The scaled boundary finite element method (SBFEM) [Song and Wolf (1997)] is a semi-analytical method combining the advantages of the finite element method (FEM) and the boundary element method (BEM). The domain consists of a small number of large-sized subdomains and only the subdomain boundaries need to be discretized. The modeled dimensions are reduced by one as the BEM, but no fundamental solutions are needed. Consequently, the FEM's flexibility and the BEM's simplicity in pre-processing and remeshing are both retained.

Polygon elements are widely used in FEM and have two attractive features. First, polygon elements are flexible in meshing domains with complex geometries such as polycrystal. Second, polygon elements generally have superior accuracy because of their high order shape functions. Recently, a versatile procedure is developed to generate polygon mesh from Delaunay triangulation and applied to static and dynamic crack propagation modeling [Ooi et al. (2012; 2013)]. It is demonstrated that the polygon scaled boundary finite element method (PSBFEM) is good at dealing with domains with complicated geometries and singularities, not only in pre-processing but also in remeshing, while the high accuracy of SBFEM is retained.

Combining the polygon subdomains with a simple remeshing procedure, a novel adaptive polygon SBFEM (APSBFEM) for elastodynamics is developed. This paper is organized as follows: Section 2 discusses the SBFEM and its solutions in time domain briefly. Section 3 presents a posteriori

energy error estimator. A simple adaptive method is described in Section 4, including the remeshing procedure and the mesh mapping algorithm, and a flowchart is given out as well. A benchmark elastodynamics problem is modeled and discussed in Section 5. Conclusions are stated in Section 6.

Methodology

The scaled boundary finite element method

A domain consists of 3 polygon subdomains is described in Figure 1(a). Figure 1(b) shows the details of Subdomain 1. The subdomain is represented by scaling a defining curve S relative to a scaling center and the entire subdomain boundary has to be visible from the scale center. A normalized radial coordinate ζ is defined, varying from zero at the scaling center and unit value on S . A circumferential coordinate η is defined around the defining curve S . A curve similar to S defined by $\zeta=0.5$ is shown in Figure 1(b). The coordinates ζ and η form a local coordinate system used in all the subdomains and simple transformation equations between the local and global Cartesian coordinates can be established through:

$$x = x_0 + \zeta \left(\frac{x_1 + x_2 - 2x_0}{2} + \frac{(x_2 - x_1)\eta}{2} \right) \quad (1)$$

$$y = y_0 + \zeta \left(\frac{y_1 + y_2 - 2y_0}{2} + \frac{(y_2 - y_1)\eta}{2} \right) \quad (2)$$

where (x_1, y_1) and (x_2, y_2) are nodal coordinates of an element on the boundary and (x_0, y_0) are the coordinates of the scaling center.

The displacements of any point (ζ, η) in a subdomain are calculated by

$$\mathbf{u}(\zeta, \eta) = \mathbf{N}(\eta)\mathbf{u}(\zeta) \quad (3)$$

where $\mathbf{u}(\zeta)$ are the displacements along the radial lines and are analytical with respect to ζ . $\mathbf{N}(\eta)$ are the shape functions in the circumferential direction which are the same as used in FEM.

The stresses in a subdomain are calculated by

$$\boldsymbol{\sigma}(\zeta, \eta) = \mathbf{D}\mathbf{B}^1(\eta)\mathbf{u}(\zeta)_{,\zeta} + \frac{1}{\zeta}\mathbf{D}\mathbf{B}^2(\eta)\mathbf{u}(\zeta) \quad (4)$$

where $\mathbf{B}^1(\eta)$ and $\mathbf{B}^2(\eta)$ are coefficient matrixes, and \mathbf{D} is the elasticity matrix.

Solutions in time domain

In elastodynamics, the equilibrium condition of a subdomain without body loads can be formulated using the virtual work statement [Yang et al. (2011)]

$$\int_{V_s} \delta \boldsymbol{\varepsilon}^T \boldsymbol{\sigma} dV - \int_{S_s} \delta \mathbf{u}^T \mathbf{t} ds + \int_{V_s} \delta \mathbf{u}^T \rho \ddot{\mathbf{u}} dV = 0 \quad (5)$$

where $\delta \boldsymbol{\varepsilon}$ is the virtual strain vector, $\delta \mathbf{u}$ the virtual displacement vector, $\boldsymbol{\sigma}$ the stress vector, \mathbf{u} the displacement vector, $\ddot{\mathbf{u}}$ the acceleration vector, ρ the material density, \mathbf{t} the traction on the boundary, V_s the volume and S_s the boundary of the subdomain.

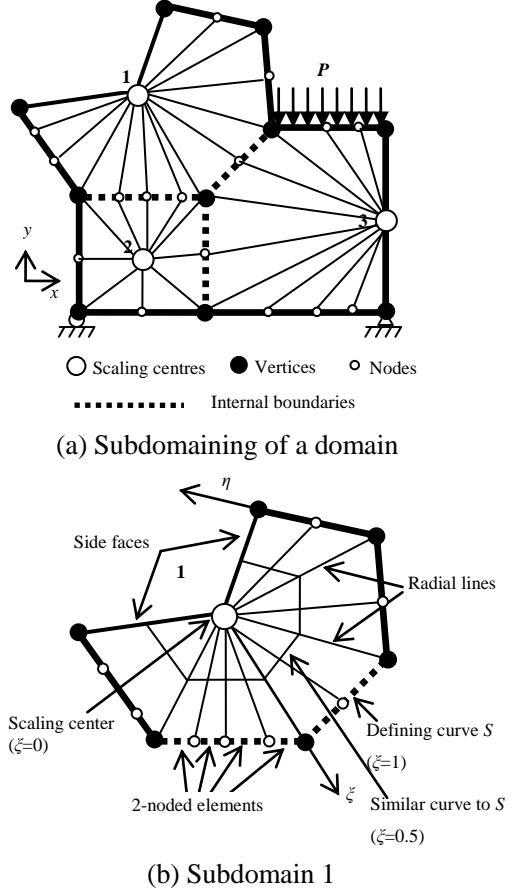


Figure 1. Concept of SBFEM

The dynamic equilibrium equation of a subdomain is derived as

$$\mathbf{M}_s \ddot{\mathbf{u}}_b + \mathbf{K}_s \mathbf{u}_b = \mathbf{p}_s \quad (6)$$

where \mathbf{u}_b is the displacement vector and $\ddot{\mathbf{u}}_b$ is the acceleration vector on the subdomain boundary, \mathbf{p}_s the subdomain load vector, \mathbf{K}_s the subdomain stiffness matrix and \mathbf{M}_s the subdomain mass matrix.

The nodal displacement vector on the subdomain boundary is

$$\mathbf{u}_b = \mathbf{\Phi} \mathbf{c} \quad (7)$$

where $\mathbf{\Phi} = \{\boldsymbol{\varphi}_1, \boldsymbol{\varphi}_2, \dots, \boldsymbol{\varphi}_N\}$ is a matrix in which the vectors $\boldsymbol{\varphi}_i$ are obtained from solving a standard eigen problem and $\mathbf{c} = \{c_1, c_2, \dots, c_N\}^T$ are constants (modal participation factors) dependent on boundary conditions, and N is the number of degrees of freedom (DOFs) of the subdomain.

Time integration scheme

Assembling Eq. (6) for all subdomains leads to the global equation system

$$\mathbf{M}\ddot{\mathbf{U}} + \mathbf{K}\mathbf{U} = \mathbf{P} \quad (8)$$

where \mathbf{M} and \mathbf{K} are the assembled global mass and stiffness matrices, \mathbf{P} the global load vector, \mathbf{U}_n and $\ddot{\mathbf{U}}_n$ the nodal displacement and acceleration vectors respectively. The Newmark integration scheme is used to solve Eq. (8) in this study and $\beta = 0.25$ and $\gamma = 0.5$ are used with unconditional stability.

The subdomain displacement field is then obtained as

$$\mathbf{u}(\xi, \eta) = \mathbf{N}(\eta) \sum_{i=1}^N c_i \xi^{\lambda_i} \boldsymbol{\varphi}_i \quad (9)$$

where λ_i ($i=1-N$) are eigen values from solving a standard eigen problem.

The stress field in the subdomain is then calculated from Eq. (4)

$$\boldsymbol{\sigma}(\xi, \eta) = \mathbf{DB}^1(\eta) \left(\sum_{i=1}^N c_i \lambda_i \xi^{\lambda_i-1} \boldsymbol{\varphi}_i \right) + \mathbf{DB}^2(\eta) \left(\sum_{i=1}^N c_i \xi^{\lambda_i-1} \boldsymbol{\varphi}_i \right) \quad (10)$$

Differentiating Eq. (9) with respect to time, the velocities and accelerations at any point in a subdomain are obtained as

$$\dot{\mathbf{u}}(\xi, \eta) = \mathbf{N}(\eta) \sum_{i=1}^N \dot{c}_i \xi^{\lambda_i} \boldsymbol{\varphi}_i \quad (11)$$

$$\ddot{\mathbf{u}}(\xi, \eta) = \mathbf{N}(\eta) \sum_{i=1}^N \ddot{c}_i \xi^{\lambda_i} \boldsymbol{\varphi}_i \quad (12)$$

The constants \dot{c}_i and \ddot{c}_i are calculated from the nodal velocities and accelerations on the subdomain boundary $\dot{\mathbf{u}}_b$ and $\ddot{\mathbf{u}}_b$ which are subsets of $\dot{\mathbf{U}}$ and $\ddot{\mathbf{U}}$, respectively, by differentiating Eq. (7) with respect to time

$$\dot{\mathbf{c}} = \mathbf{\Phi}^{-1} \dot{\mathbf{u}}_b \quad (13)$$

$$\ddot{\mathbf{c}} = \mathbf{\Phi}^{-1} \ddot{\mathbf{u}}_b \quad (14)$$

where $\dot{\mathbf{c}} = \{\dot{c}_1, \dot{c}_2, \dots, \dot{c}_N\}^T$ and $\ddot{\mathbf{c}} = \{\ddot{c}_1, \ddot{c}_2, \dots, \ddot{c}_N\}^T$.

Posteriori energy error estimator

For elastodynamic problems, the energy norm of the total energy can be estimated by

$$\|\mathbf{u}\| = \left(\|\mathbf{u}\|_k^2 + \|\mathbf{u}\|_s^2 \right)^{1/2} \quad (15)$$

where $\|\mathbf{u}\|_k$ and $\|\mathbf{u}\|_s$ are the energy norm of the kinetic energy and the strain energy respectively. NS is the number of subdomains.

Based on SBFEM, the strain energy norm can be estimated by [Zhang et al. (2011)]

$$\|\mathbf{u}\|_s \approx \left(\sum_{s=1}^{NS} \sum_{i=1}^N \sum_{j=1}^N \frac{c_i c_j}{\lambda_i + \lambda_j} \int_{S_s} \boldsymbol{\sigma}_i^*(\eta)^T \mathbf{D}^{-1} \boldsymbol{\sigma}_j^*(\eta) |J| d\eta \right)^{1/2} \quad (16)$$

where $\boldsymbol{\sigma}_i^*$ is the recovered stresses of i th mode at the boundary nodes, obtained by nodal average method for linear element here.

And the kinetic energy norm can also be evaluated semi-analytically

$$\|\mathbf{u}\|_k = \left(\sum_{s=1}^{NS} \sum_{i=1}^N \sum_{j=1}^N \frac{\rho \dot{c}_i \dot{c}_j}{\lambda_i + \lambda_j + 2} \int_{S_s} (\dot{\mathbf{u}}_i(\eta))^T \dot{\mathbf{u}}_j(\eta) |J| d\eta \right)^{1/2} \quad (17)$$

where $\dot{\mathbf{u}}_i(\eta)$ is the velocity vector of i th mode along the subdomain boundary.

Substituting Eqs. (16) and (17) into Eq. (15) yields

$$\|\mathbf{u}\| = \left(\sum_{s=1}^{NS} \sum_{i=1}^N \sum_{j=1}^N \left(\frac{\rho \dot{c}_i \dot{c}_j}{\lambda_i + \lambda_j + 2} \int_{S_s} (\dot{\mathbf{u}}_i(\eta))^T \dot{\mathbf{u}}_j(\eta) |J| d\eta + \frac{c_i c_j}{\lambda_i + \lambda_j} \int_{S_s} \boldsymbol{\sigma}_i^*(\eta)^T \mathbf{D}^{-1} \boldsymbol{\sigma}_j^*(\eta) |J| d\eta \right) \right)^{1/2} \quad (18)$$

The domain energy error can be evaluated as

$$\|\mathbf{e}\| \approx \left(\sum_{s=1}^{NS} \|\mathbf{e}\|_s^2 \right)^{1/2} \quad (19)$$

where

$$\|\mathbf{e}\|_s \approx \sum_{i=1}^N \sum_{j=1}^N \frac{c_i c_j}{\lambda_i + \lambda_j} \int_{S_s} \mathbf{e}_{\sigma_i}^*(\eta)^T \mathbf{D}^{-1} \mathbf{e}_{\sigma_j}^*(\eta) |J| d\eta \quad (20)$$

is the energy error of a single subdomain. $\mathbf{e}_{\sigma_i}^*(\eta)$ is the i th modal stress error on the boundary and calculated by

$$\mathbf{e}_{\sigma_i}^*(\eta) = \mathbf{N}(\eta) \boldsymbol{\sigma}_i^* - \mathbf{D}(\lambda_i \mathbf{B}^1(\eta) + \mathbf{B}^2(\eta)) \boldsymbol{\varphi}_i \quad (21)$$

The dynamic energy error estimator is defined as

$$\delta = \frac{\|\mathbf{e}\|}{\|\mathbf{u}\|} \times 100\% \quad (22)$$

Adaptive procedure

Remeshing

Assuming the optimized mesh is obtained when each subdomain contributes equally to the domain energy error. The average limit of the subdomain error is defined as

$$\|\mathbf{e}\|_s^{\text{lim}} = \bar{\delta} \left(\frac{\|\mathbf{u}\|^2}{NS} \right)^{1/2} \quad (23)$$

where $\bar{\delta}$ is the target error estimator of the domain.

A parameter θ is used to identify the subdomains need to be refined

$$\theta = \frac{\|\mathbf{e}\|_s}{\|\mathbf{e}\|_s^{\text{lim}}} \quad (24)$$

The polygon mesh of SBFEM is generated from a Delaunay triangular mesh by locating the scaling center at the common point of a patch of triangles and taking the centroids of these elements as the vertices of the subdomain. The readers are referred to [Ooi et al. (2012)] for details. In each time step, the following mesh refinement procedure is applied to all subdomains with $\theta > 1$, as illustrated in Fig. 2:

- (i) Locate the polygon subdomain(s) with exceeding error, i.e. $\theta > 1$, in the old mesh (Fig. 2(a));
- (ii) Find the corresponding triangles of the polygon that need to be refined in the triangular background mesh, and add midpoints on the triangles' boundaries, so that each triangle is split into four quarters (Fig. 2(b));
- (iii) Regenerate a Delaunay triangular mesh and a new polygon mesh (Fig. 2(c)). Consequently, the size of the polygon subdomain is scaled to half after one time refinement.

Considering the number of subdomains is small, the time on seeking the polygon is short. Since the remeshing procedure is actually implemented in the triangular background mesh and the topology of SBFEM is generated directly, it is more convenient and efficient than the remeshing procedure [Zhang et al. (2011)] carried out in the SBFEM mesh.

Mesh mapping

Once a new polygon mesh is obtained, nodal state variables, including displacement, velocity and acceleration, need to be transferred from the old mesh to the new one as initial conditions of the following time step. In SBFEM, these variables at any point within a subdomain or on its boundaries are directly calculated by Eqs. (9), (11) and (12). Specifically, for a point located at coordinates (x_A, y_A) in the new mesh after remeshing, the polygon subdomain in the old mesh within which the point (x_A, y_A) is located is first found. The coordinates (x_A, y_A) are then easily transformed

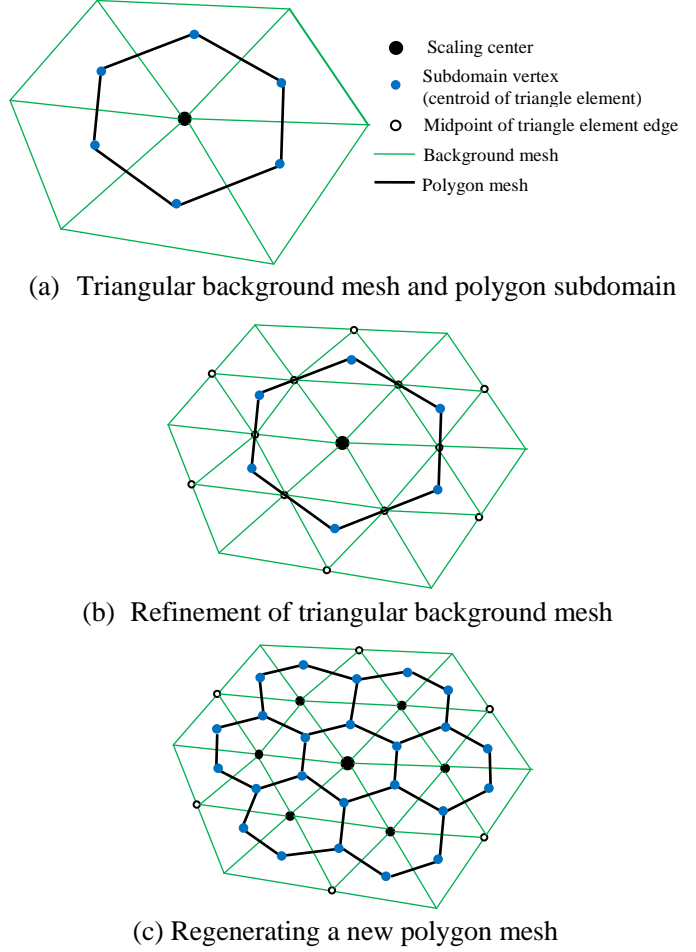


Figure 2. Remeshing procedure

to SBFEM coordinates (ζ_A, η_A) by Eqs. (1) and (2) in this polygon subdomain. The displacements, velocities and accelerations in the new mesh at Point A can be calculated as

$$\mathbf{u}_A = \mathbf{u}(\zeta_A, \eta_A) = \mathbf{N}(\eta_A) \sum_{i=1}^N c_i \zeta_A^{\lambda_i} \boldsymbol{\varphi}_i \quad (25)$$

$$\dot{\mathbf{u}}_A = \dot{\mathbf{u}}(\zeta_A, \eta_A) = \mathbf{N}(\eta_A) \sum_{i=1}^N \dot{c}_i \zeta_A^{\lambda_i} \boldsymbol{\varphi}_i \quad (26)$$

$$\ddot{\mathbf{u}}_A = \ddot{\mathbf{u}}(\zeta_A, \eta_A) = \mathbf{N}(\eta_A) \sum_{i=1}^N \ddot{c}_i \zeta_A^{\lambda_i} \boldsymbol{\varphi}_i \quad (27)$$

The flow chart

Fig. 3 illustrates the flow chart of the presented method. A parent mesh consisting of relatively large-sized polygon subdomains is generated from a Delaunay triangular mesh and a target error estimator $\bar{\delta}$ is input first. At time step n , the state variables $\mathbf{U}_n, \dot{\mathbf{U}}_n, \ddot{\mathbf{U}}_n$ are solved by the Newmark integration scheme using the old mesh at the end of time step $(n-1)$ and the error estimator δ is calculated. If δ exceeds $\bar{\delta}$, the adaptive procedure is triggered and the triangular background mesh is refined and a new polygon mesh is regenerated. The nodal state variables are then mapped from the old polygon mesh to the new one as the initial conditions. This iteration is repeated until the target is satisfied.

Numerical example

An L-shaped domain subjected to a triangular blast loading was analyzed by the adaptive method. The dimensions and material properties with SI units are shown in Fig. 4. The dynamic responses were calculated in a time period of $(0.0, 8.0\text{s})$ with a constant time increment $\Delta t=0.1\text{s}$. The element size of the triangular background mesh is 25 and totally 23 polygon subdomains are generated, as shown in Fig. 5. The target error is set as 10%.

Fig. 6(a) ~ Fig. 6(f) describe the evolution process of adaptive meshes with horizontal stresses. At the beginning of loading, steep stress gradient areas appear around the left boundary of the domain and the polygon subdomains herein are refined, whereas large-sized subdomains are used in the right area with no stress (Fig. 6(a)). With the stress wave propagates, more and more polygon subdomains are refined (Fig. 6(b) and Fig. 6(c)). In Fig. 6(d), the stress wave rebounds from the right boundary

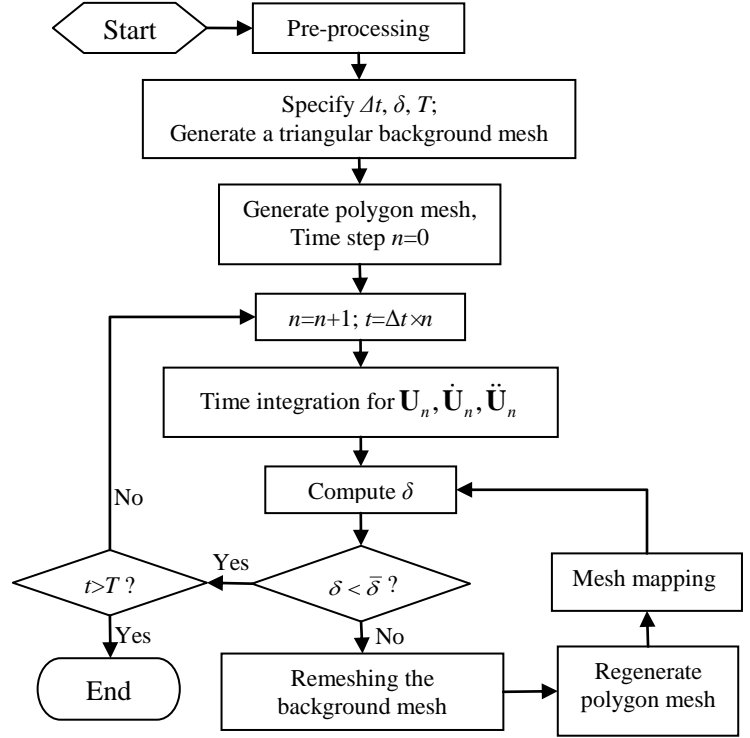


Figure 3. Flow chart of the presented method

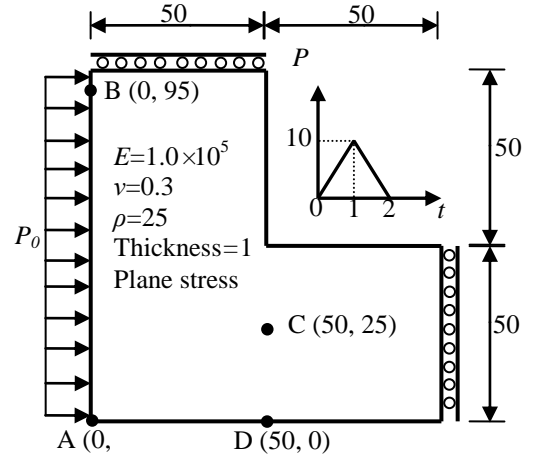


Figure 4. An L-shaped domain

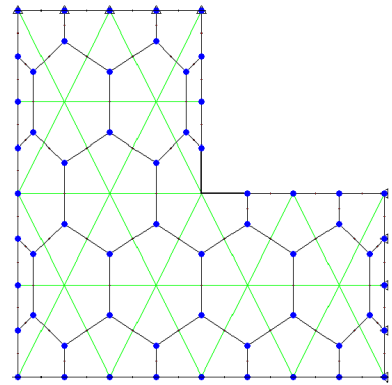


Figure 5. Parent mesh (mesh 1, DOFs=278)

and polygon subdomains near the bottom begins to be refined. Afterwards, the stress distribution becomes complicated and the steep stress gradient areas are mainly around the re-entrant corner, which has strong singularity, and very fine mesh are used, as shown in Fig. 6(e) and Fig. 6(f).

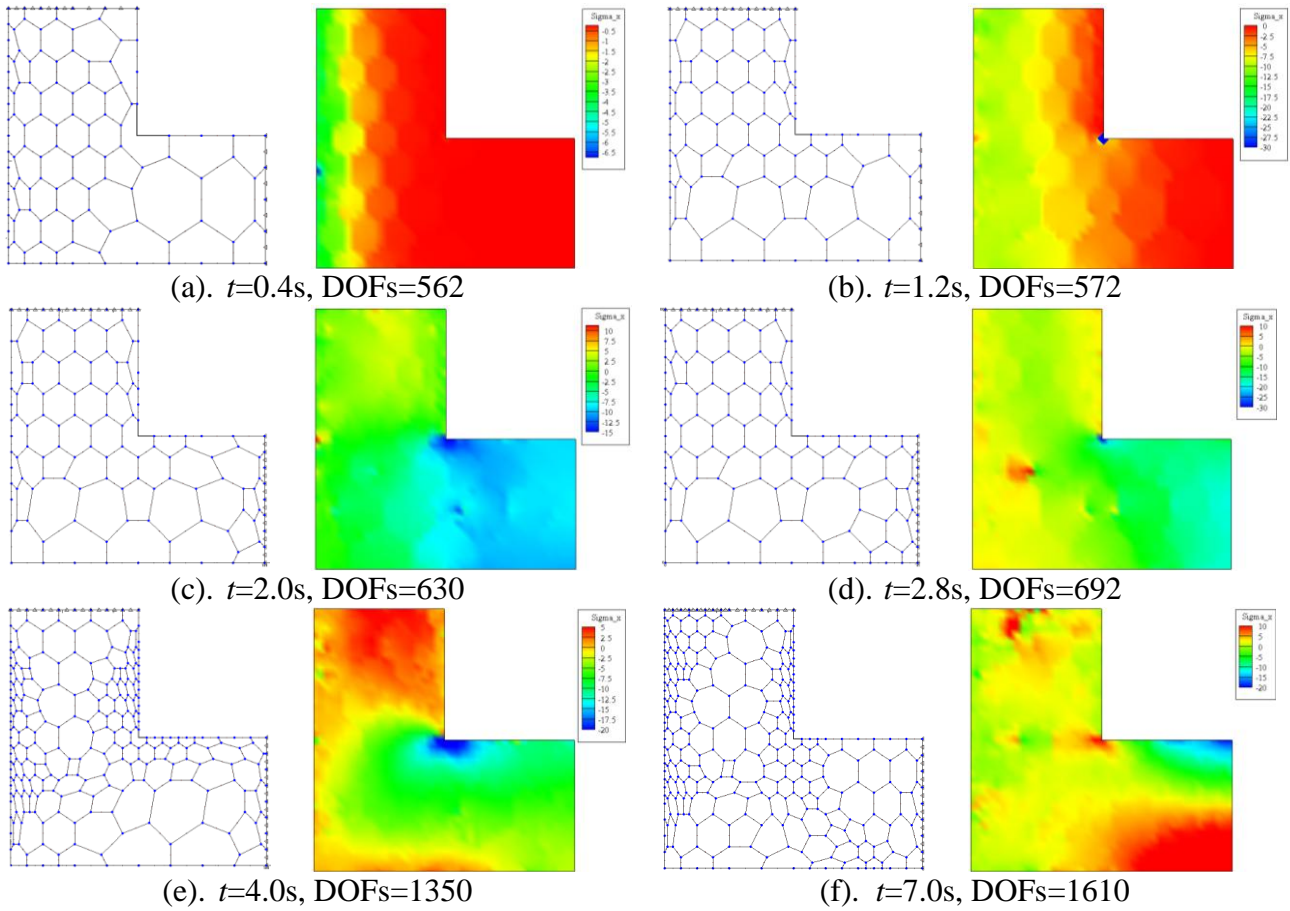


Figure 6. Adaptive meshes and evolution of horizontal stress contours

The structural dynamic responses are given out in Fig. (a) ~ Fig. (d). The results are calculated by PSBFEM based on an uniform fine mesh as shown in Fig. 7 (PSBFEM, mesh 1), an uniform coarse mesh as shown in Fig. 5 (PSBFEM, mesh 2), the presented method (PSBFEM) and AFEM proposed by [Zeng and Wiberg (1992)], respectively. It can be seen that not only displacements but also stresses of the presented method agree better with the results of AFEM than the results of PSBFEM based on uniform coarse mesh.

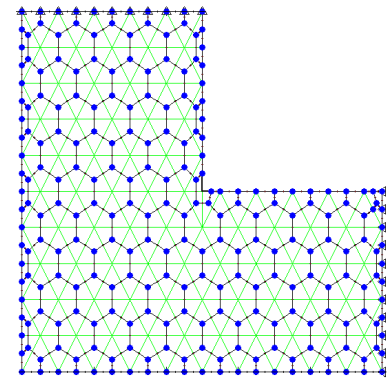


Figure 7. Fine mesh (mesh 2, DOFs=1172)

Fig. 12 records the energy error of PSBFEM using coarse mesh and the presented method. It can be seen that the value of energy error fluctuates between 6%-16% based on PSBFEM, while the error is limited under the target of 10%. Fig. 13 records the degrees of freedom (DOFs) used in the adaptive meshes.

Conclusions

An adaptive method based on polygon scaled boundary finite elements for general elastodynamic problems is developed in this study. The original and adaptive polygon meshes are generated from a triangular background mesh which is created by the Delaunay algorithm, thus the presented method

is suitable for problems with complex boundaries and cracks. The refinement is actually conducted in the background mesh so that the remeshing procedure is very convenient and straightforward. The semi-analytical energy error estimator and the simple mesh mapping algorithm endows the presented method with a good precision. It is expected to extend this method to more complicated problems, such as crack propagation.

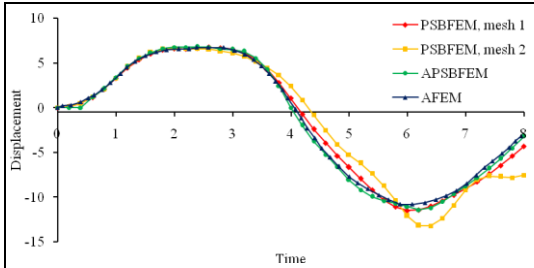


Figure 8. Horizontal displacement at A

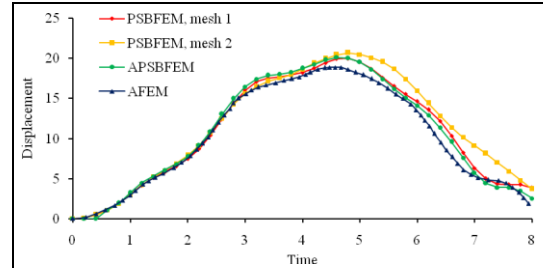


Figure 9. Horizontal displacement at B

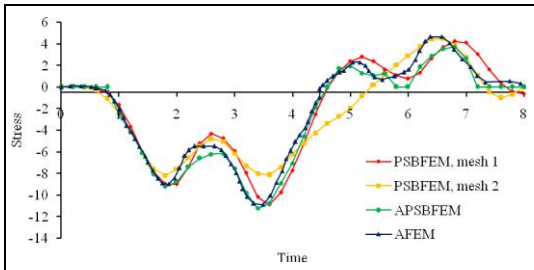


Figure 10. Horizontal normal stress at C

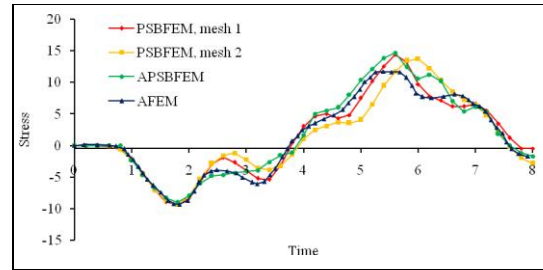


Figure 11. Horizontal normal stress at D

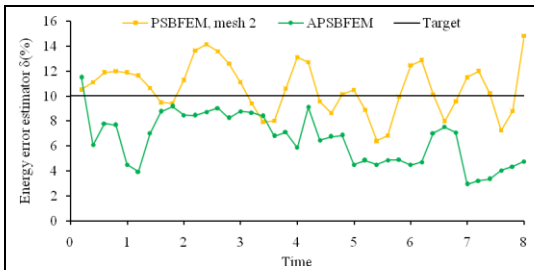


Figure 12. History of the energy error estimator

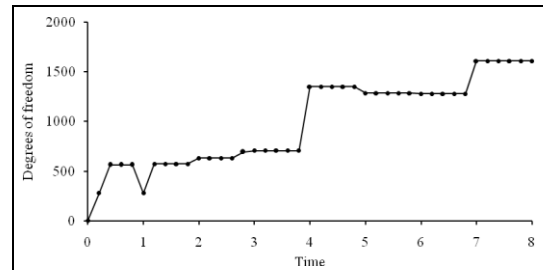


Figure 13. History of degrees of freedom

Acknowledgements

The supports of National Natural Science Foundation of China (Grant no. 51308307), Zhejiang Provincial Natural Science Foundation of China (Grant no. LQ13E080008) and Discipline Projects of Ningbo University (Grant no. xkl141044) are highly appreciated.

References

- Ooi, E. T., Shi, M., Song, C. M., Tin-Loi, F., and Yang, Z. J. (2013) Dynamic crack propagation simulation with scaled boundary polygon elements and automatic remeshing technique. *Engineering Fracture Mechanics*, **106**, 1-21.
- Ooi, E. T., Song, C. M., Tin - Loi, F., and Yang, Z. J. (2012) Polygon scaled boundary finite elements for crack propagation modelling. *International Journal for Numerical Methods in Engineering*, **91**, 319-342.
- Song, C. M. and Wolf, J. P. (1997) The scaled boundary finite-element method—alias consistent infinitesimal finite-element cell method—for elastodynamics, *Computer Methods in applied mechanics and engineering* **3**, 329-355.
- Yang, Z. J., Zhang, Z. H., Liu, G. H., and Ooi, E. T. (2011). An h -hierarchical adaptive scaled boundary finite element method for elastodynamics. *Computers and Structures* **89**, 1417-1429.

- Zeng, L. F. and Wiberg, N. -E. (1992) Spatial mesh adaptation in semidiscrete finite element analysis of linear elastodynamic problems, *Computational Mechanics* **9**, 315-332.
- Zhang, Z. H., Yang, Z. J., Liu, G. H., and Hu, Y. J. (2011) An adaptive scaled boundary finite element method by subdividing subdomains for elastodynamic problems. *Science China Technological Sciences* **54**, 101-110.